Recent Climate Change in Western Black Sea Region of Turkey by Paleoclimatic Reconstruction of Borehole Temperatures

Buğra Çelik (bugra_ce@yahoo.com)
Marmara University
Kamil Erkan
Marmara University
Mete Tayanç
Marmara University
Hakki Baltaci
Gebze Technical University
Bulent Akkoyunlu
Marmara University
Elif Balkan-Pazvantoğlu
Dokuz Eylul University

Research Article

Keywords: climate change, paleoclimate, borehole temperatures, Black Sea, Turkey

Posted Date: January 4th, 2023

DOI: https://doi.org/10.21203/rs.3.rs-2423374/v1

Version of Record: A version of this preprint was published at Pure and Applied Geophysics on September 19th, 2023. See the published version at https://doi.org/10.1007/s00024-023-03345-4.

Abstract

The impact of recent climate change varies around the world and understanding the regional variations is important for making accurate deductions and generating future climate predictions and mitigation plans. Borehole temperature reconstruction is one of the common methods to determine the ground surface temperature (GST) history of a region. In this study, high-precision (<0.01 K) borehole temperature-depth data from five different locations in Western Black Sea Region of Turkey were used for reconstruction of the ground surface temperature changes for the last century. Measurement sites are located in rural areas so the results are free from the urban heat island interference. The reconstructions reveal that ground surface temperatures have risen by an average of 0.91 °C in the study area during the last century. Results from inland sites show cooling of 0.24°C until 1975 and 0.99°C warming since then. The results in the coastal area show no such cooling period. The rapid warming trend in the last three decades revealed by GST reconstructions indicates high sensitivity of the region to present-day global warming.

1. Introduction

Climate change is a global phenomenon that impacts many aspects of the environment. Climate change increases drought risk (Diffenbaugh et al., 2015), affects lakes (Wang et al., 2018), influences the extinction rates of species (Román-Palacios and Wiens, 2020), can create conditions for disease outbreaks (Bryson et al., 2020) and increases wild fire risks (Jolly et al.,2015). The effects of climate change vary in different parts of the world. Therefore, understanding of local situation is crucial for mitigation plans. Turkey has diverse geographical features and is influenced by different teleconnection (connection of meteorological events that occur a long distance apart) patterns. These characteristics lead to different types of extreme weather events occurring around the country and climate change is increasing the frequency of those extreme weather events (Baltaci and Arslan, 2022).

Surface Air Temperature (SAT) around the globe has been rising for the last century as a result of climate change (Alexander et al., 2006; Brunet et al., 2007; Hansen et al., 2006; Ji et al.,2014; Ren et al., 2017). Rock formations at the subsurface level are affected by temperature changes occurring at the surface of the earth and hold information on surface temperature history (Pollack, 1993). This information is particularly important for understanding the climatic conditions of the earth prior to instrumental temperature recordings.

Temperature variation at the earth's surface can occur in different time periods. Night and day cycle creates the shortest temperature oscillations whereas orbital movement of the earth dictates seasonal and annual temperature trends. Surface temperature variations penetrate to subsurface layers as thermal wave and strength of this effect decline with depth exponentially as dictated by the theory of heat conduction (Birch, 1948; Pollack, 1993). Thus, ground surface temperature (GST) variations influenced by long-term climate change create temperature anomaly zones that GST history information can be extracted from by using temperature-depth profile analysis (Eppelbaum et al. 2006).

The physical conditions of the boreholes are crucial for data quality (Eppelbaum et al. 2014). Regional groundwater activity is one of the most important subjects that limits the availability of boreholes for climate reconstructions. Boreholes must have a uniform conductive heat flow originating from the depths. Vertical groundwater flows within boreholes (Erkan, 2015) also disturb this heat flow locally and prevent obtaining useful temperature-depth data from the boreholes for climate reconstructions. Canopy and manmade structures around the borehole are also important. Open space around the borehole with minimal vegetation is the ideal condition for climate studies (Pollack, 1993).

Paleoclimatic reconstruction of borehole temperatures have been applied in many different parts of the world to determine regional scale climate change. For example, Akkiriaju and Roy (2011) collected temperature-depth data from a 220-meter borehole and showed a 0.5 ± 0.1°C increase in GST over the past 92 ± 7 years in Hyderabad District of South India. Pickler et al. (2018) found a cooling period between 1850 and 1980, in their study in Northern Central Chile. According to the

study, cooling period was followed by 1.9°C increase in the last 40 years. In their study in Quebec, Canada, Chounard et al (2007) showed 1.4°C increase between mid-18th century and 1940s, followed by a 0.4°C cooling period lasted for 50 years. Following that, results showed 1.7°C increase in GST in 15 years. Correia and Safanda (2001) found in their study that about 1°C increase in GST occurred between 1950 to 1990 in Evora Town that is located in Southern Portugal. In Turkey, Erkan et al. (2019) utilized borehole paleoclimate method to determine GST values for Western and Central Anatolia. Results showed 0.33°C and 0.42°C cooling between 1900 and 1990 and warming of 1.47°C and 1.66°C between 1990 and 2010, for the western and central Anatolian sites, respectively.

In this study, reconstruction of recent GST history in six provinces of Western Black Sea Region of Turkey by using borehole temperature data was aimed. First, boreholes, which are available for measurements and have adequate depth, were identified. Then, temperature-depth (T-D) data were collected from these boreholes in the field studies. Collected T-D profiles were further analyzed to check if they were suitable for GST history reconstruction. Finally, GST histories were created by utilizing an inverse modeling algorithm.

2. Regional Setting

Western Black Sea Region of Turkey includes Kastamonu, Zonguldak, Karabuk, Bartin, Bolu and Duzce provinces (Fig. 1). In the region, mountains are oriented west-to-east, running parallel to Black Sea. This situation creates orographic effect that leads to microclimatic divisions in the area. Northern side of the mountains have warm and humid conditions, whereas the southern side have warm but step-like climatic conditions (Göktürk et al.,2011). Combination of cool northern air masses with Black Sea act as a moisture source and dictates the regional climate. The climatic difference between southern and northern side also affects ecological structure in such a way that the moist summer conditions in north allows dense forestation and prevents wild fires. Climatic and ecological diversity of the region makes it an important agriculture and forestry zone for Turkey. In our study, four of the boreholes (Akören, Devrekani, Dizdarli and Hasirli) are located in the southern (inland) parts of region and one borehole (Bartin) is located in northern (coastal) part. Borehole locations in the southern part have average elevation of 1052 meters (varying between 865 and 1185 meters) and location of the borehole in the northern part has an elevation of 42 meters.

3. Materials And Methods

3.1 Data Collection

GST history reconstructions require high-quality data obtained from boreholes. Abandoned, low yield boreholes without any mechanical attachments (pumps etc.) are readily available for temperature-depth measurements. However, only a few boreholes can provide high-quality data although they fit the description. The most common problem is the groundwater flow. Secondly, even the groundwater activity is negligible, intra-borehole vertical flow due to differences in pressure heads can disturb background thermal conditions in a borehole (Erkan, 2015). Many measurement sites had to be eliminated due to these effects.

Spatial distribution of the borehole sites used for GST modeling is shown in Fig. 1. Data collection was completed in three phases. The first phase took place in September 2020 and boreholes in Kastamonu Province were investigated. Kastamonu is the largest province in the region (13064 km^2). Among the 11 boreholes investigated in field studies, three of them yielded suitable temperature-depth profiles that were suitable for climate reconstructions. The second phase took place in September 2021, and boreholes in Bartin, Bolu, Duzce, Karabuk and Zonguldak provinces were investigated. Field studies on eight boreholes resulted in one suitable borehole in Bartin for climate reconstruction. Finally, the third phase of the study was completed in August 2022. The third phase covered Bolu and Bartin provinces with eight borehole sites.

One borehole in Bolu yielded suitable results for climate reconstruction. The borehole in Bartin which was logged in 2021 was also relogged in 2022.

As shown in Fig. 1, boreholes in Kastamonu are located in Dizdarli, Devrekani and Hasirli Districts. These districts are located in inland parts of Kastamonu province. Each location has its distinct topographic characteristics. Dizdarli is located on the western region of Kastamonu. The studied borehole is located near a village on a hill. Devrekani and Hasirli Districts are located about 20km north of Kastamonu city center, south of Kure mountains. The borehole in Hasirli is located near a village, with a vast open space around it with very light vegetation. The borehole in Devrekani is located on a small hill with no vegetation and it is 500 meters away from the farmyards. The borehole in Bartin province is located about 8 km south of the central district, in an area that is mostly grassland. It is inside an orchard that was planted in 2017. Finally, borehole in Bolu province is located near Akoren village. The village is located on an open area. The properties of the boreholes are shown in Table 1.

Table 1
Properties of the studied boreholes and sites. H: elevation, LD: logging date as month.year, BD: borehole depth, WT: depth of water table, D: borehole diameter, T_0: undisturbed GST at time = 0,λ: thermal conductivity, qb: background heat flow

Location	Latitude	Longit	H m	LD	BD m	WT m	D cm	T_0 °C	λ W/(m·K)	qb mW/m^2	Lithology
Akoren	40.9699	32.0531	865	08.22	115	15	20	12.01	2–3	32-47.5	Limestone (0-115)
Bartin	41.5633	32.3932	42	08.21	210	5	20	13.83	2–3	57.3–85.8	Marl (0-210)
Devrekani	41.6074	33.8432	1087	09.20	170	80	20	10.15	2.76 1.90	38.5	Limestone (0–48) Diorite (48–170)
Dizdarli	41.6733	32.9234	885	09.20	87.5	15	20	8.87	2–3	15.3–22.4	Limestone (0–95)
Hasirli	41.6367	33.9837	1185	09.20	95	60	20	10.27	2.89	20.79	Marble (0-110)

Temperature logging device includes a thermistor sensor that can obtain high-resolution temperature-depth data (Erkan et al., 2017). During the measurement process, temperature logging probe was released into the boreholes and temperature and depth data were recorded with 2.5–5 meter logging intervals. When the probe is in water, about 20 seconds was employed to reach equilibrium at each logging depth. On the other hand, measurements above static water level needed to be approached differently as sensitive temperature logging probe took longer to reach equilibrium in air. Therefore, a time-lapse measurement procedure was necessary for measurements above the water level. During these measurements, temperatures at each 30-sec intervals were recorded for five minutes at each depth (Fig. 2).

For extrapolation of the time-lapse temperatures to the final equilibrium temperature, the following equation was used (Costain, 1970):

$$T = T_f\left(1 - e^{-\frac{t}{\tau}}\right) + T_0 e^{-\frac{t}{\tau}}$$

where t is the time of recording, T is the temperature at time t, T_f is the final temperature, T_0 is the initial temperature and τ is the time constant of the probe (taken as 3.5 minutes for our probe). Equilibrium temperature value (T_f) was then

obtained by applying generalized least squares (GLS) method (Chapra and Canale, 2011) between the data and the equation above. For the detection and elimination of the problematic measurements, we applied a two-step procedure. First, we accepted the results at a certain depth satisfying $|T_f - T_0| \leq 0.02$ as this upper bound is within the practical limit of temperature measurements in the field. For the measurements in the remaining depths, we enforced that the standard error (SE) of the GLS fit is ≤ 5%. These thresholds were selected in compliance with the error margin used in the paleoclimatic reconstruction model discussed below.

Figure 2 shows example temperature measurements from Devrekani that were taken above the water table level. For 30 meters (Fig. 2-a), $|T_f - T_0|$ value is 0.04 which is above the threshold but SE is found as 4% which is below 5% limit. Therefore, T_f value of 10.793°C that is calculated by our algorithm is acceptable. As another example, Fig. 2-b shows temperature measurements and curve fit data from 45-meter temperature-depth log data. $|T_f - T_0|$ value here is found as 0.017 which is below the threshold so calculated value of 10.883°C is acceptable for T_f.

Temperature-depth data used as the input for GST modeling are shown in Fig. 3. Except Deverakani and Hasırlı, all data were recorded below the water table level. In the subsurface, short-term annual variations in surface temperatures are generally effective down to depths of ~ 20m (Harris and Chapman, 1998; Erkan et al., 2019). Our repeated T-D measurements in Bartin that is one year apart also showed that seasonal variations can be effective down to around 25 meters Therefore, temperature logs influenced by short-term annual temperature variations were omitted from GST model inputs.

Variations of the topography can have significant static effect on the background geothermal gradients and hence the background heat flow. The boreholes used for GST modeling are located with insignificant topography except Dizdarlı. As shown in Fig. 5, during generating the transient data (data after the static conditions are removed) the effect of topography on the background conditions are automatically eliminated. Hence, no topographic correction was applied for Dizdarlı site

3.2 GST Reconstructions

Ground surface temperature reconstructions were performed by utilizing the Functional Space Inversion (FSI) algorithm (Shen and Beck, 1991). FSI algorithm is based on functional space analysis instead of conventional discrete formulation; the solution is provided by using the iterative gradient method. FSI model requires temperature-depth profile, thermal properties of subsurface layers, background heat flow and undisturbed surface temperature as input. In our study, temperature-depth profiles were determined by instrumental loggings as described in the data collection section. Thermal properties of subsurface layers were determined by either measuring collected rock samples or using literature values based on lithological descriptions (see Table 1). Background heat flow (qb) was calculated by taking the deepest section of the temperature-depth log where temperature-depth profile shows a linear trend and can be defined as the undisturbed zone. According to Fourier's Law:

$$qb = \frac{(T_2 - T_1)}{(d_2 - d_1)} \times \lambda$$

where d_1 and d_2 are two depth points in linear portions of the temperature-depth curve, T_1 and T_2 are temperatures measured at depths d_1 and d_2 and finally, λ is the thermal conductivity (W/m/K) of the medium. Thermal conductivity values for Hasirli and Devrekani were determined by instrumental measurements of collected rock samples (Table 1) and remaining thermal conductivity values were obtained from literature after lithological identification of the collected rock samples (Gul at al., 2006, Balkan et al., 2017). In Bartin, Akoren and Dizdarli boreholes thermal conductivity values were taken as range of values due to unavailability of thermal conductivity measurements. Undisturbed surface temperatures ("pre-observational mean GST", Harris and Chapman, 1997) were determined by extending background T-D profiles (see

Fig. 3) to the surface. FSI model processes these data as inputs and produces a posteriori temperature-depth and background heat flow values. These products are used to test the model accuracy by comparing them with the observed values. If a priori and a posteriori profiles are in agreement, reconstructed GST values are accepted as the confirmed model.

4. Results

Reconstructed GST histories are shown in Fig. 4. Due to elimination of near-surface seasonal variations, very recent changes in the GST histories cannot be modeled (see Pollack, 1993) As a result of this, GST models cover 1900–2010 period. Boreholes investigated in Kastamonu province show a cooling period starting from 1900, followed by a warming period. Duration of cooling and warming periods differ in each location. Devrekani district shows 0.4°C cooling between 1900 and 1960, followed by 0.96°C warming until early 2000s. GST model shows a slight 0.15°C cooling in the late 2000s but net change from 1900 to 2010 still adds up to 0.56°C warming. In Dizdarli, a longer cooling period is found until late 20th century with 0.27°C-0.4°C. After cooling period, 0.64°C-0.9°C warming is found until 2010. Hasirli district shows 0.83°C cooling period between 1900 and late 1980s. Following the cooling period, 1.38°C warming is found until 2010. Borehole investigated in Bartin province show a different warming trend. Here, GST starts rising with the beginning of 20th century and 1.4°C-1.67°C warming is found. The result in Akoren shows similarities with Kastamonu in terms of cooling prior to warming. 0.1°C-0.3°C cooling is found until mid-20th century and it is followed by 1.4°C-1.5°C warming until 2010.

Comparison of modelled and measured T-D values after removing background T-D values is shown in Fig. 5. Modelled T-D curves are smoother because FSI model eliminates small temperature fluctuations within defined error margins to reconstruct long-term GST history. Results show that modelled and measured T-D values are in agreement. Pearson correlation analysis of measured and modelled T-D values show correlation coefficients greater than 0.97 in all boreholes.

In order to compare SAT and GST results, SAT archive data were obtained from Turkish State Meteorological Service (TSMS). Comparison of GST model results and SAT history from Kastamonu, Bartin and Bolu TSMS stations is shown in Fig. 6. SAT values are expressed as anomalies with respect to the mean of 1961–1990 period, and GST values are given as difference from pre-observational undisturbed background surface temperature. Both SAT and GST results show a significant increase in warming starting from late 20th century. In Kastamonu province SAT shows decrease until 1950s and a sharp increase starting from 1990s. Dizdarli and Hasirli GST histories show similar trends, however, late warming starts earlier in Devrekani. In Bartin, SAT recordings show sharp increase starting from late 1980 and accordingly, GST histories show that 50% of the total warming occurred in that period. Similarly, SAT recordings show increase in late 1980s in Bolu and warming in Akoren GST also increases in that period.

5. Discussion

According to our study, GST histories in Dizdarli, Devrekani, Hasirli and Akoren show two phases as 0.24°C cooling between 1900–1975 and 0.99°C warming afterwards. In a similar study in Turkey, Erkan et al. (2019) focused on Western and Central Anatolia. According to this study, GST history shows three phases. First, a small warming occurs between 1900 and 1950s which is less than 0.25°C. Following that, cooling of an average ~ 0.5°C occurs until 1990s. Finally, ~ 1.2°C warming occurs from 1990s to 2010s. Although GST histories of Western Black Sea Region show different warming/cooling trend than Western and Central Anatolian Regions, both similarly show significant warming in the late 20th century and early 21st century.

GST model of Bartin shows a different warming trend than other sites. It shows slow and steady warming starting from the early 20th century, increasing greatly in the last quarter of the century. Main geographical difference between Bartin and other locations in this study is that Bartin is located on the Black Sea side of the orographic effect. The results can also be explained by urban heat island effect due to its proximity to the center of the district as observed in other

provinces of Turkey (Tayanç and Toros, 1997). However, other non-climatic factors such as land-use change cannot be excluded for this site due to its location in a farmland.

Our results show rapid increase in GST starting from late 1990s. Projections on regional effects of climate change on the Eastern Mediterranean show that Anatolian Peninsula is among regions that will have a dramatic increase in surface temperatures (Gao and Giorgio,2008; Onol and Samazzi,2009). Studies predict that surface air temperatures in Western Black Sea Region will increase 4.5°C-5°C during 2070–2100, compared to 1961–1990 average temperature values, and are in agreement with our results.

6. Conclusion

In this study temperature-depth data from five boreholes were used to reconstruct ground surface temperature history in the Western Black Sea Region. Reconstructed GST histories starting from the year 1900 show 0.91°C increase on average from the beginning of 20th century, and it intensifies near the late 20th century. The averaged GST models show a 0.24°C cooling period between 1900 and 1975 prior to 0.99°C warming in Akoren, Devrekani, Dizdarli and Hasirli. Our study reveals the rapid warming trend in the western Black Sea region during the last decade revealed by GST reconstructions of borehole temperatures. The results indicate the sensitivity of the region to present-day global warming. The results of this study can be used in regional climate projections for this region.

Statements And Declerations

Funding

This study was supported by Marmara University, Scientific Research Commission (FDK-2020-10051) and Türkiye Ulusal Jeodezi ve Jeofizik Birliği (TUJJB) (National Union of Geodesy and Geophysics of Turkey) with project TUJJB-TUMEHAP-2020-03.

Competing Interests

The authors have no competing interests to declare that are relevant to the content of this article.

Author Contributions

All authors contributed to the study conception and design. Material preparation, data collection and analysis were performed by Buğra Çelik and Kamil Erkan. The first draft of the manuscript was written by Buğra Çelik and all authors commented on previous versions of the manuscript. All authors read and approved the final manuscript.

References

1. Akkiraju, V. V., & Roy S (2011). Geothermal climate change observatory in south India 1: Borehole temperatures and inferred surface temperature histories. *Physics and Chemistry of the Earth*, Parts A/B/C 36(16),1419–1427. https://doi.org/10.1016/j.pce.2011.01.004
2. Alexander, L. V., Zhang, X., Peterson, T. C., Caesar, J., Gleason, B., Klein Tank, A. M. G., Haylock M., Collins D., Trewin B., Rahimzadeh F., Tagipour A., Rupa Kumar K., Revadekar J., Griffiths G., Vincent L., Stephenson D. B., Burn J., Aguilar E., Brunet M., … Vazquez-Aguirre J. L. (2006). Global observed changes in daily climate extremes of temperature and precipitation. *Journal of Geophysical Research,* 111(D5). https://doi.org/10.1029/2005JD006290
3. Balkan, E., Erkan, K., & Şalk, M. (2017). Thermal conductivity of major rock types in western and central Anatolia regions, Turkey. *Journal of Geophysics and Engineering*, 14(4), 909–919. https://doi.org/10.1088/1742-2140/aa5831

4. Baltaci, H., & Arslan, H. (2022). Seasonal and regional variability of wet and dry spell characteristics over Turkey. *Atmospheric Research,* 270, 106083. https://doi.org/10.1016/j.atmosres.2022.106083
5. Birch, A. F. (1948). The effects of Pleistocene climatic variations upon geothermal gradients. *American Journal of Science,* 246(12), 729–760. https://doi.org/10.2475/ajs.246.12.729
6. Bodri, L., & Čermák, V. (1997). Reconstruction of remote climate changes from borehole temperatures. *Global and Planetary Change,* 15(1-2), 47–57. https://doi.org/10.1016/S0921-8181(97)00004-0
7. Bodri, L. and Cermak, V (2011). *Borehole climatology: a new method how to reconstruct climate*. 3rd edition. Elsevier. https://doi.org/10.1016/B978-0-08-045320-0.X5000-5
8. Brunet, M., Jones, P. D., Sigró, J., Saladié, O., Aguilar, E., Moberg, A., Della-Marta P. M., Lister D., Walther A., & López D. (2007). Temporal and spatial temperature variability and change over Spain during 1850–2005. *Journal of Geophysical Research,* 112(D12). https://doi.org/10.1029/2006JD008249
9. Bryson, J. M., Bishop-Williams K. E., Berrang-Ford L., Nunez, E. C., Lwasa, S., Namanya, D. B., & Harper, S. L. (2020). Neglected Tropical Diseases in the Context of Climate Change in East Africa: A Systematic Scoping Review. *The American Journal of Tropical Medicine and Hygiene*, 102(6), 1443–1454. https://doi.org/10.4269/ajtmh.19-0380
10. Chapra, S. C., & Canale, R. P., (2011). *Numerical methods for engineers.* Mcgraw-Hill.
11. Chouinard, C., Fortier, R., & Mareschal J.-C. (2007). Recent climate variations in the subarctic inferred from three borehole temperature profiles in northern Quebec, Canada. *Earth and Planetary Science Letters,* 263(3-4), 355–369. https://doi.org/10.1016/j.epsl.2007.09.017
12. Correia, A., & Šafanda, J. (2001). Ground surface temperature history at a single site in southern Portugal reconstructed from borehole temperatures. *Global and Planetary Change,* 29(3-4), 155–165. https://doi.org/10.1016/S0921-8181(01)00087-X
13. Costain, J. K. (1970). Probe response and continuous temperature measurements. *Journal of Geophysical Research,* 75(20), 3969–3975. https://doi.org/10.1029/JB075i020p03967
14. Diffenbaugh, N. S., Swain, D. L., Touma, D. (2015). Anthropogenic warming has increased drought risk in California. *Proceedings of the National Academy of Science.,* 112(13), 3931–3936. https://doi.org/10.1073/pnas.1422385112
15. Eppelbaum, L. V., Kutasov, I. M., & Barak, G. (2006). Ground surface temperature histories inferred from 15 boreholes temperature profiles: comparison of two approaches. *Earth Sciences Research Journal,* 10(1), 25-34.
16. Eppelbaum, L., Kutasov, I., & Pilchin, A. (2014). Thermal Properties of Rocks and Density of Fluids. *Lecture Notes in Earth System Sciences.* 99–149. https://doi.org/10.1007/978-3-642-34023-9_2
17. Erkan, K. (2015). Geothermal investigations in western Anatolia using equilibrium temperatures from shallow boreholes. *Solid Earth*, 6(1), 103–113. https://doi.org/10.5194/se-6-103-2015
18. Erkan, K., Akkoyunlu, B., Balkan, E., & Tayanç, M. (2017). A portable borehole temperature logging system using the four-wire resistance method. *Journal of Geophysics and Engineering,* 14(6), 1413–1419. https://doi.org/10.1088/1742-2140/aa7ffe
19. Erkan, K., Akkoyunlu, B., İnal, M. O., Balkan-Pazvantoğlu, E., Tayanç, M. (2019). Twentieth-century paleoclimatic modeling of borehole temperatures in western and central Anatolia regions, Turkey. *International Journal of Earth Sciences,* 108(4), 1137–1146. https://doi.org/10.1007/s00531-019-01698-7
20. Gao, X., & Giorgi, F. (2008). Increased aridity in the Mediterranean region under greenhouse gas forcing estimated from high resolution simulations with a regional climate model. *Global and Planetary Change,* 62(3-4), 195–209. https://doi.org/10.1016/j.gloplacha.2008.02.002
21. Göktürk, O. M., Fleitmann, D., Badertscher, S., Cheng, H., Edwards, R. L., Leuenberger, M., Fankhauser, A., Tüysüz, O., & Kramers, J. (2011) Climate on the southern Black Sea coast during the Holocene: implications from the Sofular Cave record. *Quaternary Science Reviews,* 30(19-20), 2433–2445. https://doi.org/10.1016/j.quascirev.2011.05.007

22. Gul, I. H., & Maqsood, A. (2006). Thermophysical Properties of Diorites along with the Prediction of Thermal Conductivity from Porosity and Density Data. *International Journal of Thermophysics,* 27(2), 614–626. https://doi.org/10.1007/s10765-005-0007-0
23. Hansen, J., Sato, M., Ruedy, R., Lo, K., Lea, D. W., & Medina-Elizade, M. (2006). Global temperature change. *Proceedings of the National Academy of Sciences*, 103(39), 14288–1429. https://doi.org/10.1073/pnas.0606291103
24. Harris, R. N., & Chapman, D. S. (1997). Borehole Temperatures and a Baseline for 20th-Century Global Warming Estimates. *Science,* 275(5306), 1618–1621. https://doi.org/10.1029/97JB03297
25. Ji, F., Wu, Z., Huang, J., & Chassignet, E. P. (2014). Evolution of land surface air temperature trend. *Nature Climate Change*, 4(6), 462–466. https://doi.org/10.1038/nclimate2223
26. Jolly, W. M., Cochrane, M. A., Freeborn, P. H., Holden, Z. A., Brown, T. J., Williamson, G. J., & Bowman, D. M. J. S. (2015). Climate-induced variations in global wildfire danger from 1979 to 2013. *Nature Communications*, 6(1). https://doi.org/10.1038/ncomms8537
27. Önol, B., & H. M. Semazzi, F. (2009). Regionalization of Climate Change Simulations over the Eastern Mediterranean. *Journal of Climate,* 22(8), 1944–1961. https://doi.org/10.1175/2008JCLI1807.1
28. Pickler, C., Gurza Fausto, E., Beltrami, H., Mareschal, J.-C., Suárez, F., Chacon-Oecklers, A., Blin, N., Cortés Calderón, M. T., Montenegro, A., Harris, R., & Tassara, A. (2018). Recent climate variations in Chile: constraints from borehole temperature profiles. *Climate of the Past*. 14(4), 559–575. https://doi.org/10.5194/cp-14-559-2018
29. Pollack, H. N. (1993). Climate change inferred from borehole temperatures. *Global and Planetary Change,* 7(1-3), 173-179. https://doi.org/10.1016/0921-8181(93)90048-S
30. Ren, Y.-Y., Ren, G.-Y., Sun, X.-B., Shrestha, A. B., You, Q.-L., Zhan, Y.-J., Rajbhandari, R., Zhang, P.-F., & Wen, K.-M. (2017). Observed changes in surface air temperature and precipitation in the Hindu Kush Himalayan region over the last 100-plus years. *Advances in Climate Change Research*, 8(3), 148–156. https://doi.org/10.1016/j.accre.2017.08.001
31. Román-Palacios, C., & Wiens, J. J. (2020). Recent responses to climate change reveal the drivers of species extinction and survival. *Proceedings of the National Academy of Sciences*, 117(8), 4211–4217. https://doi.org/10.1073/pnas.1913007117
32. Shen, P. Y., & Beck, A. E. (1991). Least squares inversion of borehole temperature measurements in functional space. *Journal of Geophysical Research: Solid Earth*, 96(B12), 19965–19979. https://doi.org/10.1029/91JB01883
33. Tayanç, M., & Toros, H. (1997). Urbanization effects on regional climate change in the case of four large cities of Turkey. *Climatic Change,* 35(4), 501–524. https://doi.org/10.1023/A:1005357915441
34. Wang, W., Lee, X., Xiao, W., Liu, S., Schultz, N., Wang, Y., Zhang, M., & Zhao, L. (2018). Global lake evaporation accelerated by changes in surface energy allocation in a warmer climate. *Nature Geoscience,* 11(6), 410–414. https://doi.org/10.1038/s41561-018-0114-8

Figures

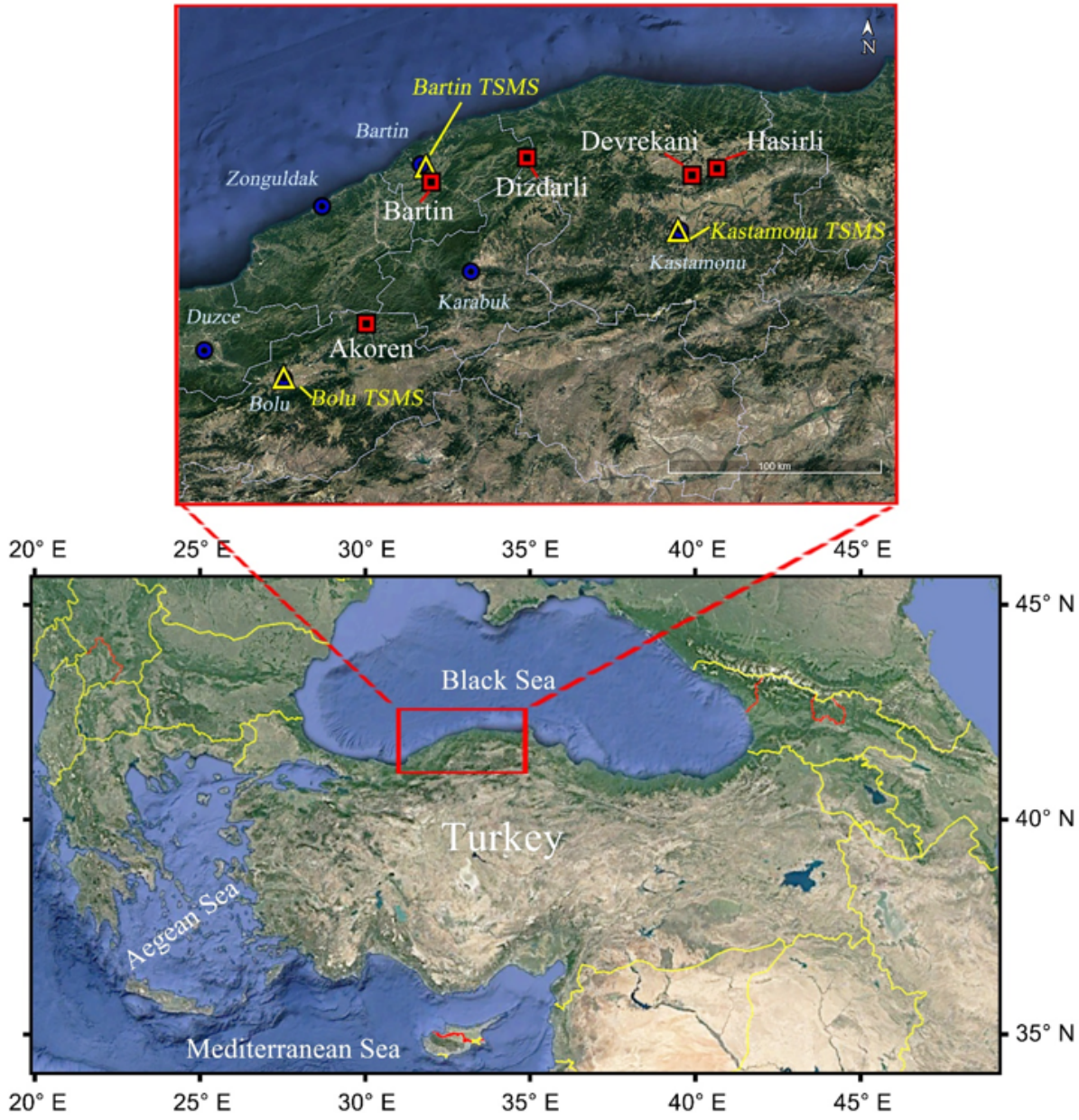

Figure 1

Map of the study area. Labels marked with red squares show borehole locations, italic labels with blue markings show province centers and yellow labels with yellow triangle markings show locations of Turkish State Meteorology Service (TSMS) stations used in this study.

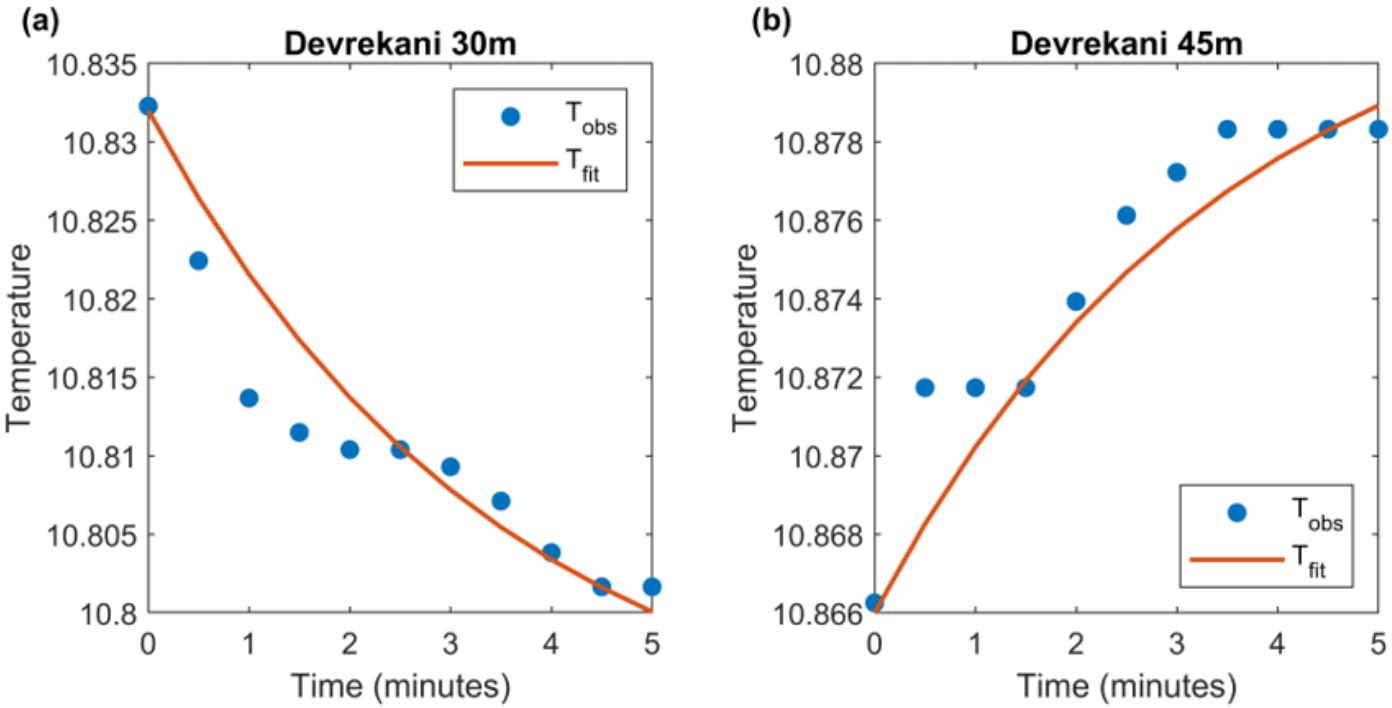

Figure 2

Time-lapsetemperature measurements and data fitting at various depths above water level.

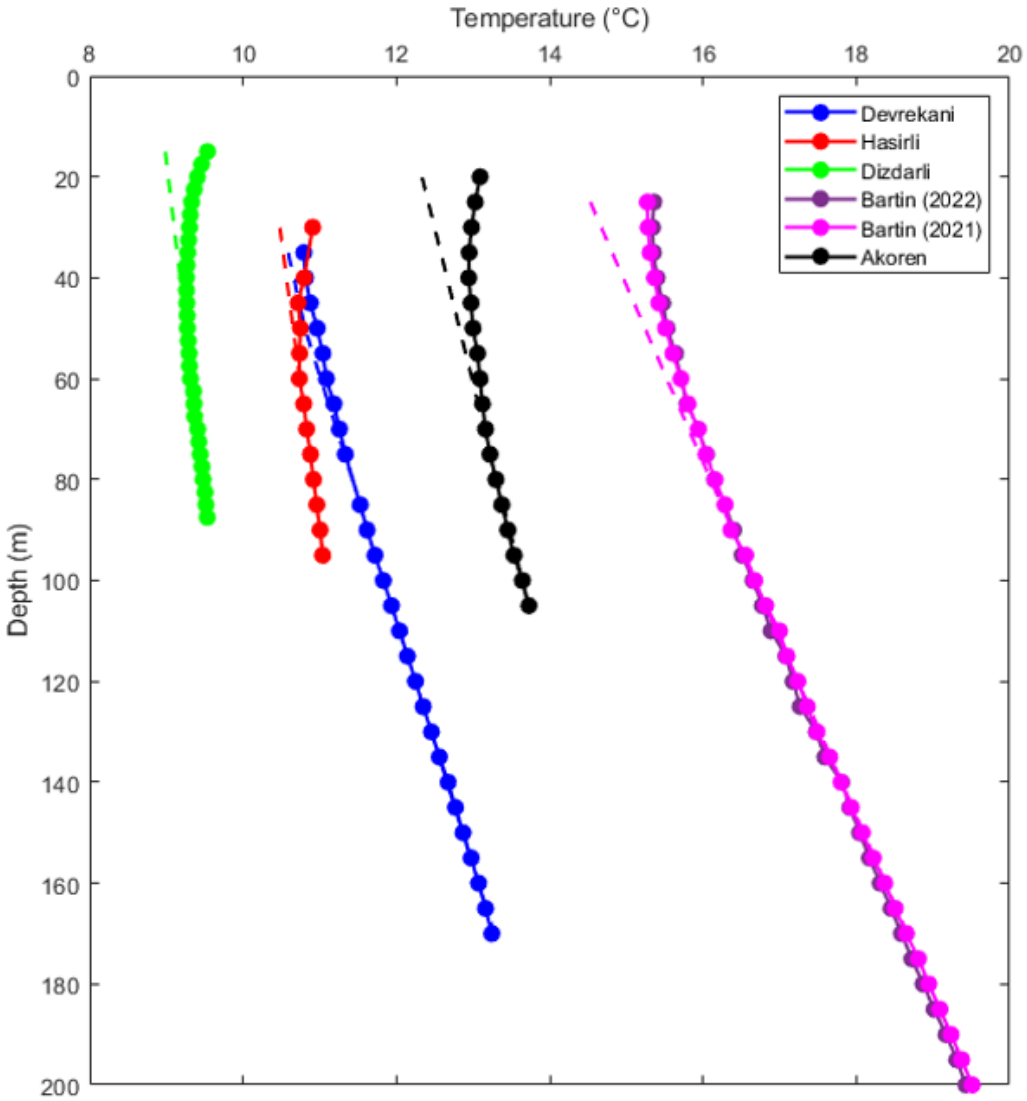

Figure 3

T-D curves of boreholes used in climate reconstruction. Water tabel levels are given in Table 1Dashed lines show background conditions. Both 2021 and 2022 measurements for Bartin is shown.

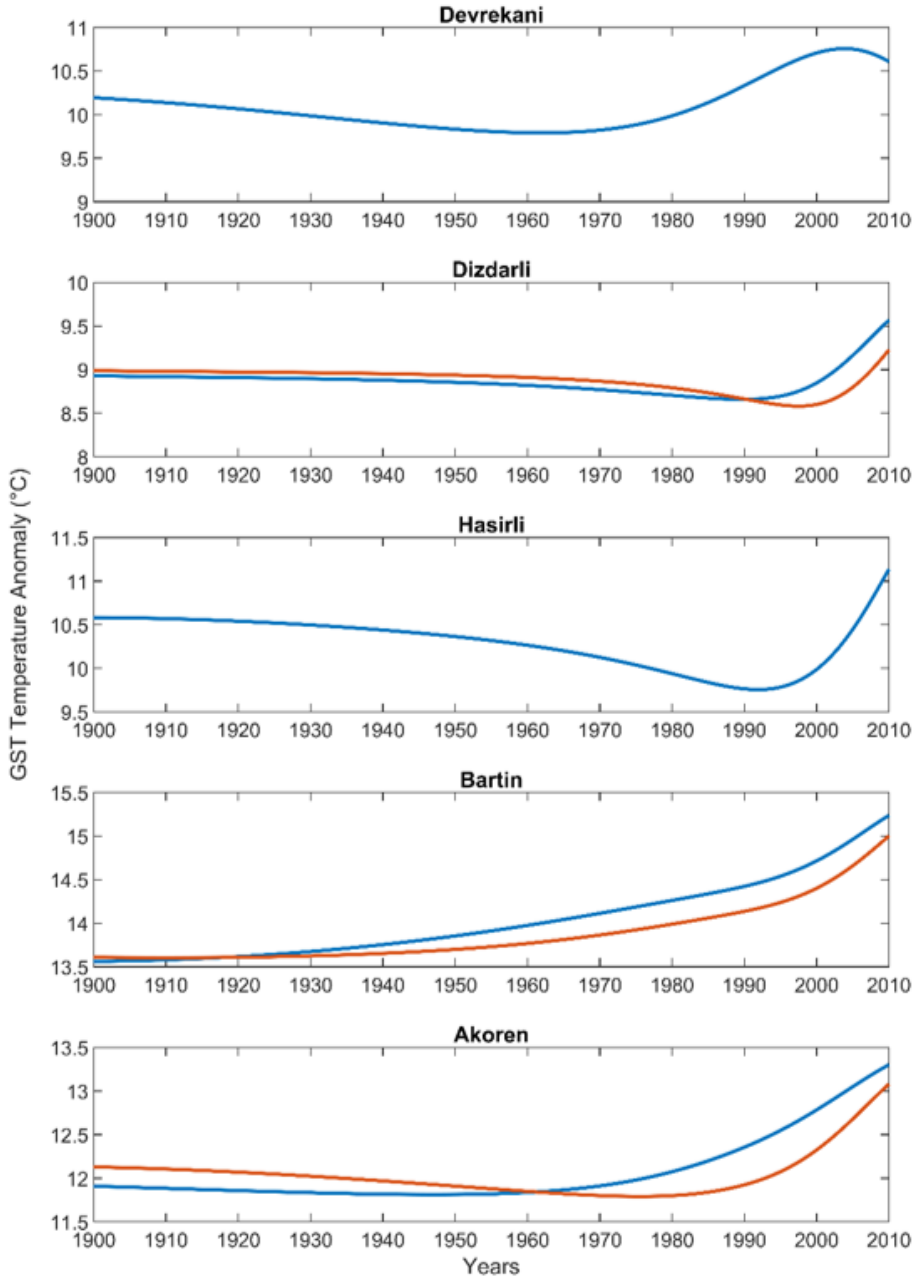

Figure 4

Reconstructed GST histories for Western Black Sea Region study sites. Akoren, Bartin and Dizdarli have upper and lower range for results due to unavailability of thermal conductivity measurements samples. In their GST plots orange lines represent λ=3 W/m/K and blue lines represent λ=2 W/m/K conditions.

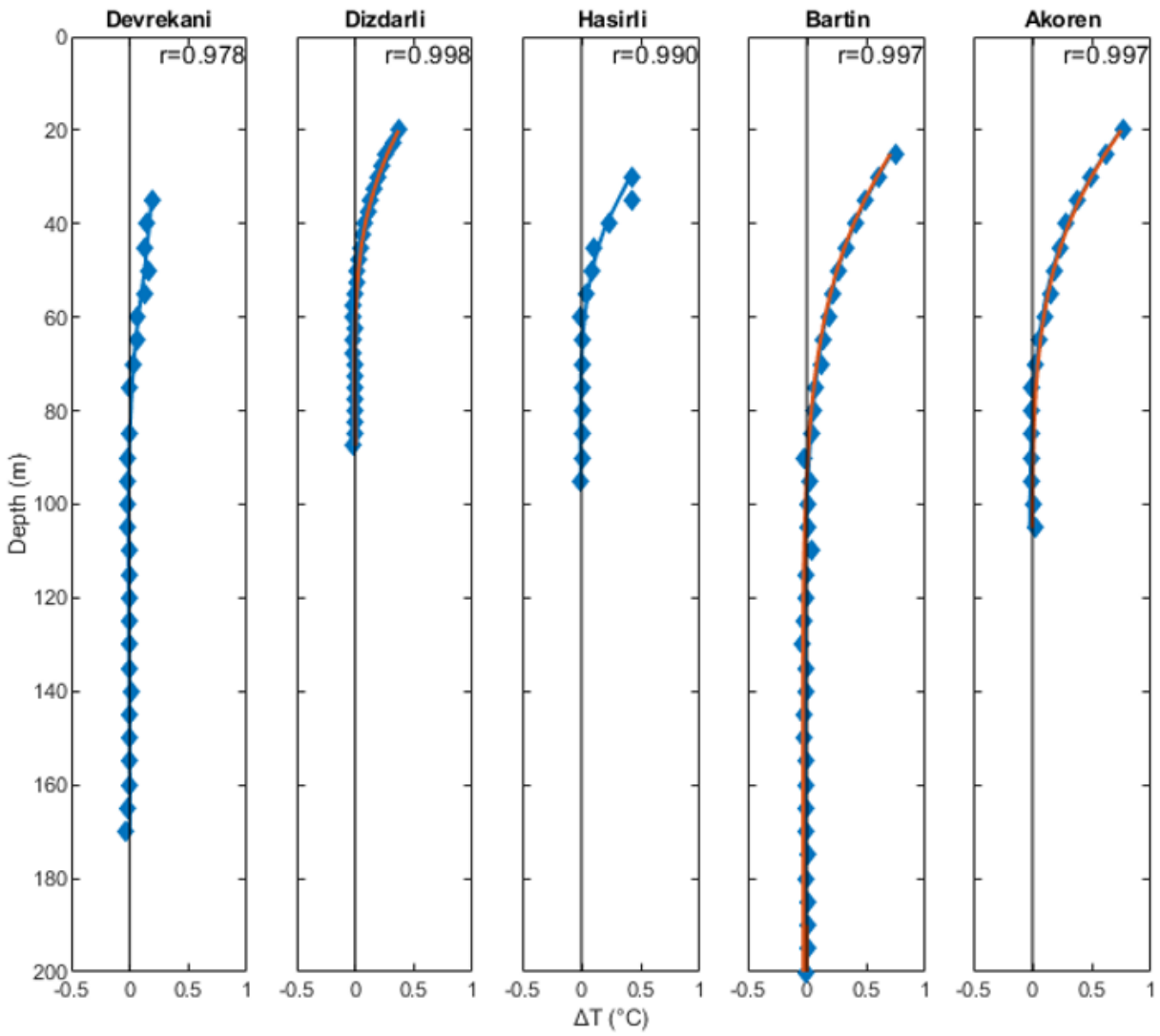

Figure 5

Measured transient temperatures (diamonds) and modelled transient temperatures (lines). For Akoren, Bartin and Dizdarli blue lines show λ=2 W/m/K and orange lines show λ=3 W/m/K conditions. Pearson correlation coefficient (r) of modelled and measured temperature profiles for each borehole is shown at the top right corner.

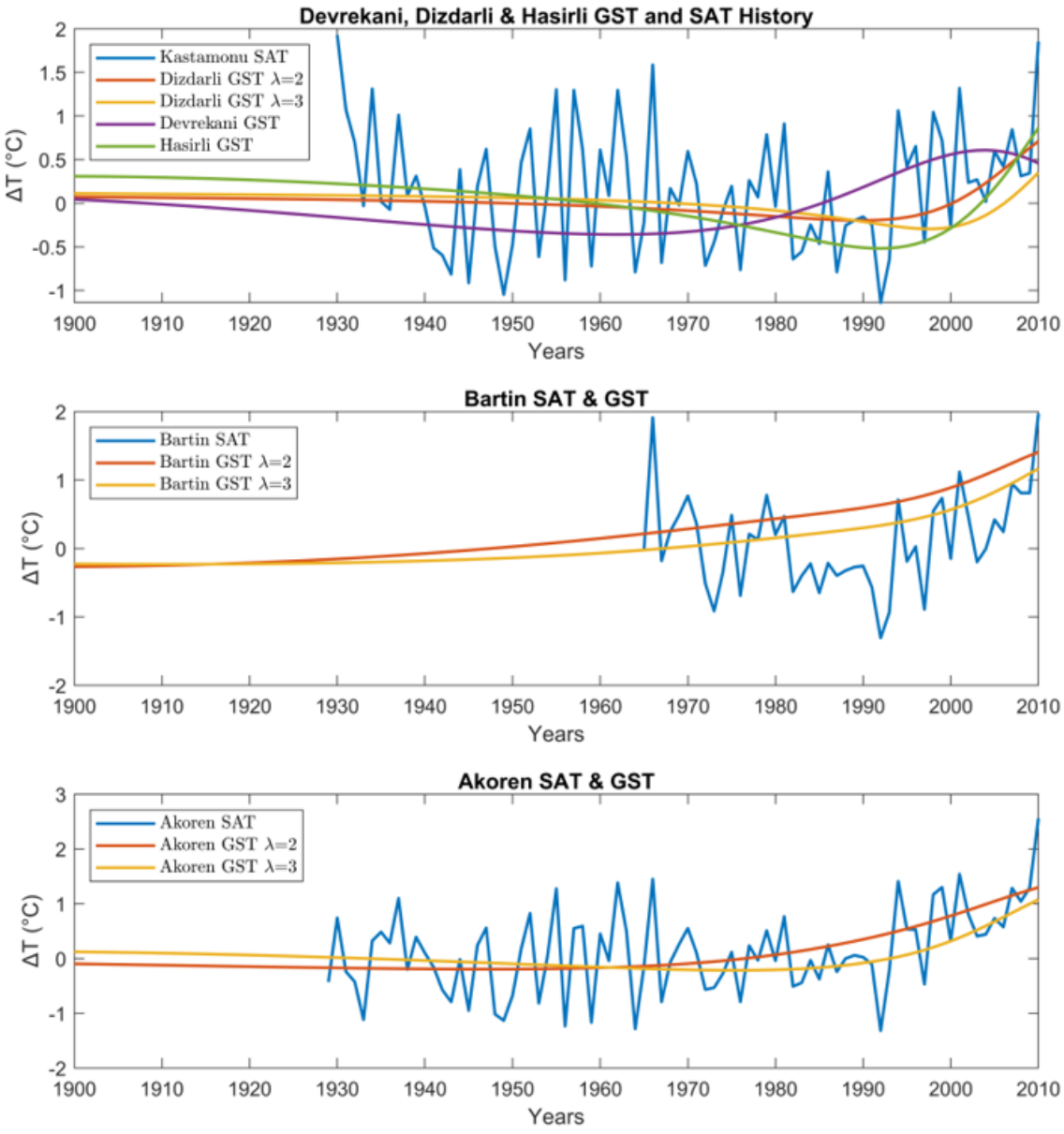

Figure 6

Comparison of reconstructed GST histories and SAT history records from TSMS stations.